Viral cell-to-cell movement requires formation of cortical punctate structures containing Red clover necrotic mosaic virus movement protein.

AUTHOR(S):

Kaido, Masanori; Funatsu, Naoko; Tsuno, Yasuko; Mise, Kazuyuki; Okuno, Tetsuro

CITATION:

Kaido, Masanori ...[et al]. Viral cell-to-cell movement requires formation of cortical punctate structures containing Red clover necrotic mosaic virus movement protein.. Virology 2011, 413(2): 205-215

ISSUE DATE:

2011-05-10

URL:

http://hdl.handle.net/2433/139997

Viral cell-to-cell movement requires formation of cortical punctate structures containing *Red clover necrotic mosaic virus* movement protein

Masanori Kaido*, Naoko Funatsu, Yasuko Tsuno, Kazuyuki Mise, Tetsuro Okuno

Laboratory of Plant Pathology, Graduate School of Agriculture, Kyoto University, Kyoto 606-8502, Japan

* Corresponding author. Mailing Address: Laboratory of Plant Pathology, Graduate School of Agriculture, Kyoto University, Sakyo-ku, Kitashirakawa, Kyoto, 606-8502, Japan. Phone: TEL: +81-75-753-6148, FAX: +81-75-753-6131. E-mail: kaido@kais.kyoto-u.ac.jp

Abstract

Movement protein (MP) of *Red clover necrotic mosaic virus* (RCNMV) forms punctate structures on the cortical endoplasmic reticulum (ER) of *Nicotiana benthamiana* cells, which are associated with viral RNA1 replication (Kaido et al., Virology 395, 232-242. 2009). We investigated the significance of ER-targeting by MP during virus movement from cell to cell, by analyzing the function of a series of MPs with varying length deletions at their C-terminus, either fused or not fused with green fluorescent protein (GFP). The C-terminal 70 amino acids were crucial to ER-localization of MP-GFP and cell-to-cell movement of the recombinant virus encoding it. However, C-terminal deletion did not affect MP functions, such as increasing the size exclusion limit of plasmodesmata, single-stranded RNA binding *in vitro*, and MP interacting *in vivo*. We discuss the possible role of this MP region in virus movement from cell to cell.

Key words: cell-to-cell movement, endoplasmic reticulum, replicase complex, positive-strand RNA virus, *Dianthovirus*

Introduction

Plant viruses encode one or more movement proteins (MPs). The principal role of MP is to transport viral genomes or virions to neighboring uninfected cells through plasmodesmata (PD) and to uninfected leaves through vasculatures. These are accomplished through the interaction of MPs with ancillary viral proteins and host factor proteins (Harries and Nelson, 2008; Lucas, 2006). Structures and amino acid sequences of MPs are highly variable, but MPs all share the ability to localize at PD and increase the size exclusion limit (SEL) of PD (Benitez-Alfonso et al., 2010; Lucas, 2006; Melcher, 1990, 2000; Waigmann et al., 2004), which enables the passage of MPs complexed with viral genomes or virions.

Various MPs have been shown to localize at the endoplasmic reticulum (ER) and cytoskeletal elements, as well as PD (Harries et al., 2010). These cellular components are used in intracellular transport systems, so it seems probable that viruses use such a system for targeting of MPs to PD. Microprojectile bombardment of plasmids encoding fusion MPs with green fluorescent protein (MP-GFP), or inoculation of recombinant viruses expressing MP-GFP, has shown that several kinds of MPs localize at ER membranes, including those categorized in the 30K superfamily, triple gene block (TGB) family and double gene block family (Genovés et al., 2009, 2010; Verchot-Lubicz et al., 2007; Waigmann et al., 2004). *Tobacco mosaic virus* (TMV) includes an MP belonging to the 30K superfamily and recent studies suggest that the MP, or viral RNA, targets PD via the ER/actin and/or the microtubule network (Boyko et al., 2007; Sambade et al., 2008; Wright et al., 2007). Other researchers propose that TMV MP is targeted to PD by diffusion in the ER (Guenoune-Gelbart et al., 2008). The importance of the ER membrane in virus cell-to-cell movement has also been shown in *Potato virus X* (PVX) and *Potato mop-top virus*, where TGB proteins form ER-derived granular vesicles that are essential for virus movement from cell to cell (Haupt et al., 2005, Ju et al., 2005, 2007; Tilsner et al., 2010; Verchot-Lubicz et al., 2007, 2010).

TMV MP-GFP and PVX TGBp3-GFP colocalize with viral replicase component proteins on the cortical ER-derived vesicles, known as ‘viral replication complex (VRC)’ or ‘membrane bound bodies’, respectively (Asurmendi et al., 2004; Bamunusinghe et al., 2009; Heinlein et al., 1998; Kawakami et al., 2004). VRCs of either TMV or its close relative *Tomato mosaic virus* have been shown to move along actin filaments and target

PD independent of the ER-to-Golgi transport pathway (Christensen et al., 2009; Kawakami et al., 2004; Liu et al., 2005; Tagami and Watanabe, 2007; Wright et al., 2007). These results, and the involvement of the TMV replicase component protein 126K in cell-to-cell movement (Hirashima and Watanabe, 2001, 2003), suggest that the processes of viral RNA replication and movement might be functionally linked.

Red clover necrotic mosaic virus (RCNMV) is a positive-strand RNA virus with a bipartite genome and belongs to the genus *Dianthovirus* in the family *Tombusviridae*. RNA1 encodes two N-terminal overlapping nonstructural proteins (p27 and p88), both of which are the essential components of the viral replicase complex (Mine et al., 2010a, 2010b; Iwakawa et al., 2011) and the coat protein (CP). CP is expressed from subgenomic RNA transcribed via the interaction of genomic RNA1 and RNA2 (Sit et al., 1998). RNA2 encodes a 35 kDa MP belonging to the 30K superfamily, which is required for virus movement between cells (Lommel et al., 1988; Xiong et al., 1993). The fact that CP is dispensable for cell-to-cell movement (Xiong et al., 1993), and that MP has the ability to bind single-stranded nucleic acids (Giesman-Cookmyer and Lommel, 1993; Osman et al., 1992, 1993) suggests that RCNMV cell-to-cell movement occurs in the form of viral RNA-MP complexes. Microinjected RCNMV MP can increase the SEL of PD and enable transport of coinjected viral RNA to neighboring cells (Fujiwara et al., 1993). Using an MP-GFP fusion protein expressed through a recombinant RCNMV it was determined that targeting of MP to PD was required for viral intercellular movement (Tremblay et al., 2005).

We have recently reported the subcellular localization of RCNMV MP-GFP in *Nicotiana benthamiana* epidermal cells and protoplasts (Kaido et al., 2009). When MP-GFP was expressed transiently, in the absence of other viral components, it localized exclusively in the cell wall. This suggests that other viral components are not essential for MP transportation to PD. MP-GFP expression from a viral construct led to formation of punctate structures with viral replicase component protein p27 on the cortical ER. It also localized to the cell wall. Transiently expressed MP-GFP also localized to punctate structures on the cortical ER in association with replication of viral RNA1, but not viral RNA2. These results suggest that RCNMV MP is recruited to the cortical ER by the viral replicase complexes formed with RNA1. Such a recruitment mechanism might help the MP to acquire viral genomic RNA1 that does not code for MP, leading to efficient cell-to-cell movement of RNA1.

We employed MP-GFP fusions to examine the role of cortical punctate structures in virus intercellular transport. The C-terminal region of the RCNMV MP is rich in hydrophilic residues (Fig. 1B) and was the focus of our study, because it is possibly exposed to the surface of the molecule, which might mean it interacts with cellular and viral components. Deletion by degrees of more than 66 amino acids deprived the MP-GFP of both the ability to form cortical punctate structures on the ER and to support cell-to-cell movement of the encoding recombinant virus. Localization to the cortical ER was significantly delayed for GFP fused with MP, where the C-terminal 70 amino acids were deleted (MPdC70-GFP), as was cell-to-cell movement of the encoding recombinant virus. There was no effect on MPdC70 localization to the cell wall, enlargement of PD SEL, binding to single-stranded RNA or interaction with MP *in vivo*. These results suggest that localization of RCNMV MP to cortical punctate structures on the ER is required for the viral cell-to-cell movement.

Results

Deletions of greater than 66 amino acids in the C-terminus of RCNMV MP affect cell-to-cell movement of encoding recombinant viruses

In this study, we used recombinant RCNMV to express MP-GFP. A mixture of *in vitro* transcripts of pUCR1-MsG (R1-MsG, Kaido et al., 2009, Fig. 1) and pRNA2fsMP (R2fsMP, Tatsuta et al., 2005, Fig. 1) was inoculated onto *N. benthamiana*. R2fsMP was included in the inoculum, because it is required for expression of subgenomic RNA encoding MP-GFP (Sit et al., 1998). The recombinant virus can move from cell to cell, because MP-GFP possesses the movement function (Kaido et al., 2009; Tremblay et al., 2005).

94.6% of fluorescent foci detected by epifluorescence microscopy in leaves mechanically inoculated with a mixture of R1-MsG and R2fsMP, at 30 hours post inoculation (hpi) were composed of multiple cells (Figs. 2A, left panel and B). We investigated whether the C-terminal region of RCNMV MP contributes to the viral intercellular movement, by introducing 10, 20, 30, 40, 50, 60 and 70 codon deletions to the 3′-terminal region of the MP gene in pUCR1-MsG. Deletions of up to 60 amino acids from the C-terminal did not affect cell-to-cell movement of recombinant virus at 30 hpi (Fig. 2A, middle panel and data not shown), whereas 70 amino acid deletions from the C-terminal severely affected movement. 74.9% of fluorescent foci by the inoculation of a mixture of *in vitro* transcripts from pUCR1-MdC70sG (Fig. 1, R1-MdC70sG) and R2fsMP were composed of a single cell (Figs. 2A, right panel and B), suggesting that the cell-to-cell movement function of the MPdC70-GFP was impaired.

The distinct phenotypes of the MPdC60-GFP and MPdC70-GFP led us to investigate how intermediate sizes of C-terminal deletions might affect cell-to-cell movement of recombinant viruses. A mixture of R1-MsG and R2fsMP, or separate *in vitro* transcripts from pUCR1-MdCnsG (R1-MdCnsG, n = 66 to 70, Fig. 1) and R2fsMP were inoculated onto *N. benthamiana* and the ratio of multiple cell-fluorescence was measured at 30 hpi. As the C-terminal deletion became larger, the ratio of multiple fluorescent foci decreased gradually from 86.2%, in leaves inoculated with a mixture of R1-MdC66sG and R2fsMP, down to 46.1% with R1-MdC69sG and R2fsMP, and reached to 25.1%

with R1-MdC70sG and R2fsMP (Fig. 2B). These results suggest that no single critical amino acid residue in the MP C-terminal region from 66 to 70 amino acids regulates competence for cell-to-cell movement of recombinant virus. We also confirmed that a ten amino acid deletion alone, in the MP C-terminal from 61 to 70 amino acid residues (R1-Md248sG, Fig. 1A), does not affect cell-to-cell movement of the recombinant virus (Fig. 2B), which suggests that the C-terminal 70 amino acids as a whole are important for the viral intercellular movement.

Deletions of more than 66 amino acids in the C-terminus of RCNMV MP affect ER-localization of the MP-GFP

Based on confocal laser scanning microscopy, we previously reported that RCNMV MP-GFP forms punctate structures on the cortical ER in recombinant virus-infected *N. benthamiana* epidermal cells (Kaido et al., 2009). These cytoplasmic punctate structures were also detected by using epifluorescence microscopy (Fig. 2A, left panel) and we observed that far fewer cytoplasmic punctate structures were detected in fluorescent foci with MPdC70-GFP, compared with MP-GFP or MPdC60-GFP at 30 hpi (Fig. 2A, compare right panel with other two panels). These results led us to investigate whether C-terminal deletions in the MP-GFP affect formation of cytoplasmic punctate structures. We inoculated recombinant viral RNA transcripts to *N. benthamiana* leaves and used epifluorescence microscopy to observe cytoplasmic punctate structures at 14 to 16 hpi, which is an early stage of infection when all fluorescent foci were composed of single cells. Cytoplasmic punctate structures were detected in all fluorescent cells of leaves inoculated with a mixture of R1-MsG and R2fsMP (Figs. 3A, left panel and B). The ratio of fluorescent cells where cytoplasmic punctate structures were detected gradually decreased by deleting more than 66 amino acids in the MP C-terminus, until it reached nearly 30% after deletion of the C-terminal 70 amino acids (Figs. 3A, middle panel and B). The number of cytoplasmic punctate structures with MPdC70-GFP in these foci was much lower than with MP-GFP (Fig. 3A, compare middle and left panels). No cytoplasmic punctate structures were detected in the remaining 70% of cells (Fig. 3A, right panel).

We identified the subcellular localization of MP-GFP and MdC70-GFP by confocal laser scanning microscopy. As previously reported (Kaido et al., 2009), numerous

fluorescent punctate structures were detected in the cell wall and the cortical cytoplasmic region after inoculation with a mixture of R1-MsG and R2fsMP at 14 hpi (Fig. 3C, left panel). In contrast, when leaves were inoculated with a mixture of R1-MdC70sG and R2fsMP, only lower number of smaller sized fluorescent punctate structures was detected in the cortical cytoplasmic region, whereas in the cell wall, numerous large fluorescent spots were detected at 14 hpi (Fig. 3C, middle panel). At 24 hpi and later, we detected substantial numbers of cells containing numerous cortical punctate structures with MPdC70-GFP (Fig. 3C, right panel), although the size of punctate structures was small when compared with MP-GFP.

To determine the subcellular localization of the cortical punctate structures with MPdC70-GFP, we constructed ER-localizing marker pBIC/ER-mCherry (see Materials and Methods). Typical reticulate pattern of cortical ER was detected in the cortical region of *N. benthamiana* cells agroinfiltrated with pBIC/ER-mCherry by confocal microscopy (data not shown). Cortical punctate structures formed by MPdC70-GFP colocalized with the ER-mCherry (Fig. 3D). In these cells rather distorted pattern of cortical ER was observed (Fig. 3D, middle panel), probably because viral replication induced morphological changes of ER.

These results suggest that MPdC70-GFP retains the ability to localize at punctate structures on the cortical ER, but the localization is significantly impeded.

Deletion of the C-terminal 70 amino acids of RCNMV MP does not affect the protein accumulation level of MPdC70-GFP or the recombinant virus RNA in N. benthamiana protoplasts

Reduced fluorescence in the cortical ER by the MPdC70-GFP might have resulted from a reduced replication level of the recombinant virus, or lower stability of MPdC70-GFP, and led to reduced cell-to-cell movement of the recombinant virus. Thus, we inoculated mixtures of R1-MdC70sG and R2fsMP, or R1-MsG and R2fsMP, into protoplasts of *N. benthamiana*. Fluorescent punctate structures began to appear near the protoplast surface at 12 to 14 hpi, with both treatments. MP-GFP and MPdC70-GFP were both below the detection limit by western blot analysis at this time point, using antibody against GFP (data not shown). Fluorescent punctate structures with MPdC70-GFP were generally smaller at 17 to 20 hpi and the outer boundaries of the

punctate structures appeared more ambiguous than fluorescent punctate structures with MP-GFP (Fig. 4A). Northern blot analysis of protoplasts at 20 hpi showed the accumulation of similar amounts of negative-strand RNA1 and RNA2 (Fig. 4B). Western blot analysis showed that the accumulated level of MPdC70-GFP was about 1.8-fold higher, compared with MP-GFP (Fig. 4C). This result suggests that the stability of MPdC70-GFP is relatively higher than MP-GFP. The reduced level of cell-to-cell movement and the reduced number of fluorescent punctate structures on the cortical ER of *N. benthamiana* epidermal cells with MPdC70-GFP (Figs. 2 and 3) might indicate that the protein had less affinity to cortical ER, but this is not supported by a lower accumulation of protein (discussed later).

Deletion of the C-terminal 70 amino acids of RCNMV MP does not alter the ability of the MP to increase the SEL of PD, bind single-stranded RNA or interact with MP

MPdC70-GFP localized at the cell wall of *N. benthamiana* epidermal cells (Fig. 3C), but it is possible that deletion of the C-terminal 70 amino acids deprived the protein of the ability to enlarge the PD SEL, leading to reduced cell-to-cell movement. Thus, we performed particle bombardment experiments and introduced pUBsGFP (Fig. 1), which expressed free GFP via a *Cauliflower mosaic virus* 35S promoter, together with a vector control plasmid pUBP35 (Takeda et al., 2005), into *N. benthamiana* epidermal cells. At 24 h post bombardment, 91.7% of fluorescent foci were restricted to single cells. Fluorescence was detected in two or more epidermal cells for the remaining 8.3% of foci (Fig. 5), probably due to diffusion of GFP into neighboring cells (Tamai and Meshi, 2001b). Cobombardment of pUBsGFP with pUBRMP (Fig. 1), expressing wild-type MP of RCNMV, raised the ratio of multicellular fluorescence to 54.7% (Fig. 5). Similar results (53.7%) were obtained by cobombardment of pUBsGFP with pUBRMPdC70 (Fig. 1) expressing MPdC70 (Fig. 5). Thus, the PD SEL enlargement ability of MPdC70 is similar to that found in the wild-type MP in *N. benthamiana* cells.

RCNMV is hypothesized to move from cell-to-cell in the form of a viral RNA-MP complex (Giesmann-Cookmyer and Lommel, 1993: Osman et al., 1992, 1993; Xiong et al., 1993). We conducted an RNA-binding assay to investigate the effect of C-terminal 70 amino acid deletion of MP binding of viral genomic RNA. N-terminally 6 × histidine-tagged MP or MPdC70 were overexpressed in *Escherichia coli* transformed

with pRAMP-15b or pRAMPdC70-15b (Fig. 1A), respectively, and purified using an Ni-NTA column. We used 200 nucleotide-*in vitro* transcripts of ^{32}P-labeled RCNMV RNA2 as a probe. We found that both proteins bound *in vitro* transcripts in a cooperative manner, with similar efficiency (Fig. 6), suggesting that C-terminal 70 amino acids do not play a role in MP binding to single-stranded RNA.

It was reported that three MPs that were defective for RCNMV cell-to-cell movement were complemented for this function by wt MP and one of these defective MPs, by expression of a second non-functional MP altered in a different position (Tremblay et al., 2005). This suggests that RCNMV MP forms a homopolymer and functions in virus movement. Thus we investigated whether deletion of the C-terminal 70 amino acids affects the interaction between MPs *in vivo*. We conducted a coimmunoprecipitation analysis using C-terminal myc-tagged MP (MP-myc), MPdC70 (MPdC70-myc), and C-terminal hemagglutinin (HA)-tagged MP (MP-HA), MPdC70 (MPdC70-HA), and GFP (GFP-HA) as the negative control. *N. benthamiana* leaves were agroinfiltrated with different combinations of plasmids expressing HA- and myc-tagged proteins. Both MP-HA and MPdC70-HA were detected in the precipitation experiment using anti-myc antibody (Fig. 7, lanes 1, 2, 4 and 5). When MP-HA or MPdC70-HA was expressed singly, these proteins were not detected after immunoprecipitation (Fig. 7, lanes 3 and 6). GFP-HA was not detected in the precipitation (Fig.7, lanes 7 to 9), thereby excluding the possibility of nonspecific copurification. Similar results were obtained by immunoprecipitation using anti-HA antibody (data not shown). These results indicate that RCNMV MPs interact with each other *in vivo* and that deletion of C-terminal 70 amino acids did not affect this interaction.

Discussion

We have previously hypothesized, on the basis of the subcellular localization of RCNMV MP-GFP, that RCNMV MP is recruited by viral replicase complexes formed on RNA1 to interact with an RNA1 molecule that does not code for MP (Kaido et al., 2009). According to this hypothesis, MP localization to cortical punctate structures is a crucial step in the process of virus movement from cell to cell. In this study, we found that the MP C-terminal 70 amino acid region is responsible for localization of MP-GFP to cortical punctate structures at an early stage of infection, which correlates with virus movement between cells (Figs. 2 and 3). Further characteristics of MPdC70 were similar to the wild-type MP, including localization to the cell wall (Fig. 3C), PD SEL enlargement in *N. benthamiana* epidermal cells (Fig. 5), single-stranded RNA binding *in vitro* (Fig. 6) and self-interaction competence *in vivo* (Fig. 7). Taken together, these results indicate that MP localization to punctate structures on the cortical ER is required for efficient cell-to-cell movement of RCNMV. MP occurrence in close proximity to the viral replicase complexes could lead to increased concentrations of MP and viral RNA localized in a cellular compartment, thereby facilitating both molecules to encounter.

A recent study of fluorescently labeled TMV genomic RNA localization in tobacco trichome cells shows that the viral RNA replication process is linked with the cell-to-cell movement process (Christensen et al., 2009). This study found that an initial pool of microinjected viral RNAs did not move from cell-to-cell and only the progeny viral RNA molecules synthesized in the VRCs were transported to neighboring cells. In addition, transgenically expressed TMV MP did not promote cell-to-cell movement of the injected viral RNA. These results suggest the importance of the formation of VRCs for efficient cell-to-cell movement of TMV. In contrast, several microinjection studies with *Cucumber mosaic virus* (CMV) (Ding et al., 1995; Nguyen et al., 1996), PVX (Lough et al., 1998) and RCNMV (Fujiwara et al., 1993) found that replication of viral RNA is not required for the cell-to-cell movement of viral RNA. In these experiments, however, high concentrations of MP were purified from *E. coli* and mixed with *in vitro* transcripts of viral RNA prior to injection. These experimental conditions might have enabled MP and viral RNA to form nucleoprotein complexes, thus leading to efficient cell-to-cell movement without viral RNA replication.

A correlation between localization of viral MP to vesicular structures on the cortical ER and the viral cell-to-cell movement has been suggested for PVX TGBp2 and TGBp3 (Krishnamurthy et al., 2003; Mitra et al., 2003; Ju et al., 2007, 2008). Several recombinant PVXs encoding mutant TGBp2 or TGBp3 cannot localize at the ER membrane, or granular vesicles, and failed to move from cell-to-cell, which suggests that subcellular localization of PVX MPs to the cortical ER is essential to viral movement. PVX replicase protein colocalizes with TGBp3 on the cortical ER (Bamunusinghe et al., 2009), so PVX TGBp3 protein might be recruited by the viral replicase complexes as found with RCNMV.

Infection of recombinant TMV expressing a fusion protein of C-terminal 55 amino acid-deleted MP and GFP resulted in the loss of cortical ‘inclusion bodies’ by the MP-GFP (Boyko et al., 2000). However, TMV MP with a C-terminal 55 amino acid deletion still supported virus cell-to-cell movement, but with reduced efficiency compared with the wild-type MP (Boyko et al., 2000; Gafny et al., 1992). These results suggest that the formation of a cortical inclusion body contributes to cell-to-cell movement of TMV to some degree, but that it is not essential. TMV MP is an integral membrane protein (Brill et al., 2000; Fujiki et al., 2006), so the mutant TMV MP might still have the ability to localize at the ER membrane and VRCs. However, RCNMV MP has low affinity for the ER membrane (Kaido et al., 2009), which means that the formation of large cortical punctate structures, containing the viral replicase complexes, might be a requirement for transport of viral genomic RNA.

Numerous viral MPs belonging to the 30K superfamily possess C-terminal regions that are rich in hydrophilic amino acid residues. Deletion, or alanine-scanning mutation, in the C-terminal region of several MPs showed that this region is not essential for cell-to-cell movement. For example, more than 33 amino acids in the C-terminus of *Alfalfa mosaic virus*, *Brome mosaic virus* and CMV MPs are nonessential for virus cell-to-cell movement (Nagano et al., 1997, 2001; Sánchez-Navarro and Bol, 2001; Takeda et al., 2004). These viruses belong to the family *Bromoviridae* and they require both MP and cognate CP for efficient cell-to-cell movement. The C-terminal regions of these MPs are hypothesized to interact with their cognate CPs and ensure specific transport of their virions or viral RNA-MP-CP complex. We have not yet determined whether RCNMV MP and CP interact *in vivo* via the MP C-terminal region. However,

this seems unlikely because, like TMV, RCNMV does not require CP for cell-to-cell movement (Xiong et al., 1993).

There is wide amino acid sequence diversity among strains in the C-terminal region of RCNMV MP. The N-terminal 236 amino acids of RCNMV Australian (Aus) strain MP (317 amino acids in total) used in this study shares 92.3% identity with that of the TpM-34 strain (326 amino acids), whereas the C-terminal 81 amino acids of Aus MP shares less than 50% identity with the C-terminal 90 amino acids of TpM-34 MP (Osman et al., 1991b). The naturally occurring isolate TpM-341, which expresses a mutant MP where the C-terminal 88 amino acids are replaced by 34 different amino acids, was found to exhibit restricted necrotic lesions on inoculated leaves of cowpea, whereas TpM-34 exhibited chlorotic lesions and systemic movement (Osman et al., 1991a). This suggests that MP C-terminal 88 amino acids are not essential for cell-to-cell movement of the RCNMV TpM34 strain, but they may be involved in systemic infection and/or suppression of antivirus responses by cowpea plants. Further lines of evidence using alanine-scanning mutant MP of RCNMV (Aus strain) bear out this scenario; six types of MPs, or MP-GFPs, with alanine-scanning mutations in the C-terminal 76 amino acid region supported virus movement between cells in *N. benthamiana* (Giesman-Cookmyer and Lommel, 1993; Tremblay et al., 2005), whereas three out of the six mutant MPs did not support systemic infection in host plants (Wang et al., 1998). The inability of mutant MPs to support virus systemic movement might be due to a delay in cell-to-cell movement. The MP of the TpM-341 strain (238 plus nonviral 34 amino acids) may have a delayed phenotype for cortical ER localization and cell-to-cell movement. Our preliminary results show that GFP fused to C-terminal 80 amino acid-deleted MP from Aus strain (237 amino acids) (MPdC80-GFP) resulted in both reduced number and smaller size of cortical fluorescent punctate structures, with reduced cell-to-cell movement compared with MPdC70-GFP (data not shown). The variable C-termini of RCNMV MPs might have evolved because of their nonessential requirement for cell-to-cell movement and as a result of adaptation to a variety of host proteins involved in the replication complex.

Materials and Methods

Plasmid construction

All the primers used in this study are listed in Table 1. pUCR1-MsG is described in Kaido et al. (2009). MP gene fragments with C-terminal deletions were amplified by PCR using BamRAMP5′ and RMdCn (n = 10, 20, 30, 40, 50, 60, 66, 67, 68, 69, 70 and 80) primers and pUCR1-MsG as the template. They were digested using ClaI/NheI and inserted into the ClaI/NheI sites of pUCR1-MsG to create pUCR1-MdCnsG (n = 10, 20, 30, 40, 50, 60, 66, 67, 68, 69, 70 and 80).

pUCR1-Md248sG expressing the 10 (C-terminal 61 to 70) amino acid-deleted MP fused with GFP was constructed as follows. MP fragments were amplified by PCR using primers BamRAMP5' and RMd248L, or primers RMd248R and sGFP100L, respectively, and pUCR1-MsG as the template. These fragments were mixed and used as the template for recombinant PCR using primers BamRAMP5' and sGFP100L to amplify MP gene with the 10 amino acid deletion. The fragment was digested with ClaI/NheI and inserted into the ClaI/NheI site of pUCR1-MsG to create pUCR1-Md248sG.

ER-localizing signal peptide was amplified using primers BamER5′ and mChER-L, with pUC-mGFP5-ER (Carette et al., 2000) as the template. The mCherry gene was amplified using primers ERmCh-R and KpnERmCh-L, with pmCherry-N1 (Clontech, Mountain View, CA, USA) as the template. These fragments were mixed and used as the template for recombinant PCR using primers BamER5′ and KpnERmCh-L to amplify the mCherry gene with an ER-localizing signal. The fragment was digested with BamHI and KpnI and inserted into the BamHI/KpnI site of pBICP35 (Mori et al., 1992) to create pBIC/ER-mCherry.

The BamHI/EcoRI fragment of pBICRMsG (Kaido et al., 2009) containing the MP-GFP gene was inserted into the BamHI/EcoRI site of pUBP35 (Takeda et al., 2005) to create pUB/RMsG. pUB/RMsG was digested with BamHI/ClaI and the larger fragment was treated with T4 DNA polymerase and self-ligated to create pUBsGFP.

The MP-GFP or MPdC70-GFP gene was amplified by PCR using primers BamRAMP5′ and EcoRMP/Cter or primers BamRAMP5′ and EcoRMPdC70/Cter, respectively, with pUCR1-MsG as the template. They were digested with BamHI/EcoRI

and inserted into the BamHI/EcoRI site of pUBP35 to create pUBRMP and pUBRMPdC70, respectively.

RCNMV MP gene fragments were amplified by PCR using primers RAMP5′NdeI and RAMP3′B or primers RAMP5′NdeI and BamRMPdC70Cter, respectively, and pBICRMsG as the template. The MP gene fragments were digested with BamHI and NdeI and inserted into the BamHI/NdeI site of pET-15b (Novagen, Madison, WI, USA), to create pRAMP-15b and pRAMPdC70-15b. The 5′ end of RCNMV RNA2 was amplified by PCR using EcoRI/T7 and Bam/R2-195L primers and pRC2|G (Xiong and Lommel, 1991) as the template. The amplified 200-base fragment was digested with BamHI and EcoRI and inserted into the BamHI/EcoRI site of pUC119 (Takara Bio, Otsu, Japan) to create pUCR2-200/5′.

RCNMV MP or MPdC70 genes were amplified using primers BamRAMP5′ and Eco/HA/MP-L or primers BamRAMP5′ and Eco/HA/MPdC70-L, respectively, with pUCR2 as the template. HA-tagged MP or the MPdC70 gene was digested with BamHI and EcoRI and inserted into the BamHI/EcoRI site of pBICP35 to create pBICRMP-HA or pBICRMPdC70-HA, respectively. Likewise, pBICRMP-myc or pBICRMPdC70-myc was constructed using an Eco/myc/MP-L or Eco/myc/MPdC70-L primer, respectively. The GFP gene was amplified using primers BamGFP5′ and Eco/HA/GFP-L, with pBICGFP (Takeda et al., 2005) as the template. The HA-tagged GFP gene was digested with BamHI and EcoRI and inserted into the BamHI/EcoRI site of pBICP35 to create pBICGFP-HA.

Plant growth conditions

N. benthamiana plants were grown on commercial soil (Tsuchi-Taro, Sumirin-Nosan-Kogyo Co. Ltd., Tobishima, Aichi, Japan) at 25 ± 2 °C and 16 hour illumination per day. Five-week-old plants were used for viral RNA inoculation and six-week-old plants were used for particle bombardment. Eight-week-old plants were used for the preparation of protoplasts.

Protoplast preparation and viral RNA inoculation using polyethylene glycol

N. benthamiana protoplasts were prepared and inoculated with viral RNA transcripts as described in Kaido et al. (2009).

Microscopy

GFP fluorescence was observed using an epifluorescent microscope (Axioskop; Carl Zeiss, Jena, Germany) and image capture used a CoolSNAP camera (Nippon Roper Co., Chiba, Japan).

GFP and mCherry fluorescence were observed using an Olympus FluoView FV500 confocal microscope (Olympus Optical Co., Tokyo, Japan) equipped with an argon laser and a 60 × Plan Apo oil immersion objective lens (numerical aperture 1.4). Samples were excited with the argon laser for GFP and the He:Ne laser for mCherry. We used a dichroic mirror, DM488/543, a beam splitter, SDM560, and two emission filters: BA505-525 for GFP and BA560IF for mCherry. In experiments for detecting dual localization, scanning was performed in sequential mode to minimize signal bleed-through.

All images shown are from optical sections taken at 1 μm intervals processed using Adobe Photoshop CS3 software.

Western and northern blot analyses

Protein extraction and western blot analyses were performed as described by Takeda et al. (2005). Total RNA extraction from *N. benthamiana* leaves or protoplasts and northern blot analysis were performed as described by Mizumoto et al. (2003). Probes used for detection of negative-strand RCNMV RNA1 and RNA2 were as described by Mizumoto et al. (2006). The signals were detected with a luminescent image analyzer (LAS 1000 plus; Fuji Film Co. Ltd., Tokyo, Japan) and the signal intensities were quantified using the Image Gauge program version 3.1 (Fuji Film).

Microprojectile bombardment

A microprojectile bombardment assay was performed using a PDS1000 helium particle gun (Bio-Rad, Richmond, CA, USA) following the conditions described in Tamai and Meshi (2001a).

In vitro RCNMV MP binding assay to RNA2

RCNMV MP and MPdC70 were expressed in the BL21(DE3) strain of *E. coli* using pET-15b vector (Novagen). Plasmid DNAs were transformed into E. coli cells and the resultant fresh colonies were transferred into 15 ml LB culture medium. The culture was grown to an OD_{600} of 0.6 and then induced with the addition of isopropyl β-D-thiogalactopyranoside at 0.4 mM. After 3.5 h of incubation at 37 °C, the cells were harvested and resuspended in 3 ml of HMK buffer (20 mM Tris-HCl pH 7.5, 100 mM NaCl, 12 mM $MgCl_2$, 0.1% v/v NP40). Cells were disrupted by sonication before cell debris was pelleted and dissolved with 1.5 ml of Urea buffer (0.1 M $NaH_2PO_4{\cdot}2H_2O$, 0.01 M Tris-HCl, 8 M urea, pH 8.0). After centrifugation at 10,000 × g for 30 min, the supernatant was mixed with 150 µl of Ni-NTA agarose (QIAGEN, Tokyo, Japan) and then rotated gently at room temperature for 60 min. Ni-NTA agarose was pelleted and washed with 1 ml of Urea buffer (pH 6.3) twice, then with 125 µl of Urea buffer (pH 5.9) four times, and finally eluted with 125 µl of Urea buffer (pH 4.5) five times. The elute was processed with sequential dialysis against 300 ml each of B3, B2 and B1 buffer (Giesman-Cookmyer and Lommel, 1993) for 30 min. The protein concentration was determined using the modified Bradford assay (Bio-Rad).

Probe RNA was transcribed from BamHI-digested pUCR2-200/5′ in the presence of [α-^{32}P] UTPs (800 Ci/mol, MP Bio Japan K. K., Tokyo, Japan) and purified using a Sephadex G-50 fine column (Life Technologies, Carlsbad, CA, USA).

The *in vitro* binding assay was performed essentially as described by Giesman-Cookmyer and Lommel, (1993). The labeled probe (1 ng) was incubated with 0.1–2.0 µg of MP or MPdC70 on ice for 30 min and electrophoresed on 0.75% agarose/TBE gel. The gel was dried at 80 °C for two hours and exposed to an imaging plate. Radioactive signals were detected using FLA-5100 (Fuji Film).

Coimmunoprecipitation analysis

N. benthamiana plants and *Agrobacterium tumefaciens* GV3101 (pMP90) were used for infiltration experiments as previously described by Takeda et al. (2005). *A. tumefaciens* transformed with pBICRMP-HA, pBICRMPdC70-HA or pBICGFP-HA was used for expression of HA-tagged MP, MPdC70 and GFP, respectively. *A. tumefaciens* transformed with pBICRMP-myc or pBICRMPdC70-myc was used for

expression of myc-tagged MP and MPdC70, respectively. pBICP35 was used as the vector control. Coimmunoprecipitation analysis was as described in Mine et al. (2010b).

References

Asurmendi, S., Berg, R. H., Koo, J. C. and Beachy, R. N. 2004. Coat protein regulates formation of replication complexes during tobacco mosaic virus infection. Proc. Natl. Acad. Sci. U.S.A. 101: 1415–1420.

Bamunusinghe, D., Hemenway, C. L., Nelson, R. S., Sanderfoot, A. A., Ye, C. M., Silva, M. A. T., Payton, M. and Verchot-Lubicz, J. 2009. Analysis of potato virus X replicase and TGBp3 subcellular locations. Virology 393: 272–285.

Benitez-Alfonso, Y., Faulkner, C., Ritzenthaler, C. and Maule, A. J. 2010. Plasmodesmata: Gateways to local and systemic virus infection. Mol. Plant-Microbe Interact. 23: 1403–1412.

Boyko, V., Hu, Q., Seemanpillai, M., Ashby, J. and Heinlein, M. 2007. Validation of microtubule-associated *Tobacco mosaic virus* RNA movement and involvement of microtubule-aligned particle trafficking. Plant J. 51: 589–603.

Boyko, V., van der Laak, J., Ferralli, J., Suslova, E., Kwon, M-O. and Heinlein, M. 2000. Cellular targets of functional and dysfunctional mutants of Tobacco mosaic virus movement protein fused to green fluorescent protein. J. Virol. 74: 11339–11346.

Brill, L. M., Nunn, R. S., Kahn, T. W., Yeager, M. and Beachy, R. N. 2000. Recombinant tobacco mosaic virus movement protein is an RNA-binding, α-helical membrane protein. Proc. Natl. Acad. Sci. U.S.A. 97: 7112–7117.

Carette, J. E., Stuiver, M., Van Lent, J., Wellink, J. and Van Kammen, A. 2000. Cowpea mosaic virus infection induces a massive proliferation of endoplasmic reticulum but not golgi membranes and is dependent on de novo membrane synthesis. J. Virol. 74: 6556–6563.

Chiu, W., Niwa, Y., Zeng, W., Hirano, T., Kobayashi, H. and Sheen, J. 1996. Engineered GFP as a vital reporter in plants. Curr. Biol. 6: 325–330.

Christensen, N., Tilsner, J., Bell, K., Hammann, P., Parton, R., Lacomme, C. and Oparka, K. 2009. The 5′ cap of Tobacco mosaic virus (TMV) is required for virion attachment to the actin/endoplasmic reticulum network during early infection. Traffic 10: 536–551.

Ding, B., Li, Q., Nguyen, L., Palukaitis, P. and Lucas, W. J. 1995. Cucumber mosaic virus 3a protein potentiates cell-to-cell trafficking of CMV RNA in tobacco plants. Virology 207: 345–353.

Emini, E. A., Hughes, J. V., Perlow, D. S. and Boger, J. 1985. Induction of hepatitis A virus-neutralizing antibody by a virus-specific synthetic peptide. J. Virol. 55:836–839.

Fujiki, M., Kawakami, S., Kim, R. W. and Beachy, R. N. 2006. Domains of tobacco mosaic virus movement protein essential for its membrane association. J. Gen. Virol. 87: 2699–2707.

Fujiwara, T., Giesman-Cookmeyer, D., Ding, B., Lommel S. A. and Lucas, W. J. 1993. Cell-to-cell trafficking of macromolecules through plasmodesmata potentiated by the Red clover necrotic mosaic virus movement protein. Plant Cell 5: 1783–1794.

Gafny, R., Lapidot, M., Berna, A., Holt, C. A., Deom, C. M. and Beachy, R. N. 1992. Effects of terminal deletion mutations on function of the movement protein of Tobacco mosaic virus. Virology 187: 499–507.

Genovés, A., Navarro, J. A. and Pallás, V. 2009. A self-interacting carmovirus movement protein plays a role in binding of viral RNA during the cell-to-cell movement and shows an actin cytoskeleton dependent location in cell periphery. Virology 395: 133–142.

Genovés, A., Navarro, J. A. and Pallás, V. 2010. The intra- and intercellular movement of *Melon necrotic spot virus* (MNSV) depends on an active secretory pathway. Mol. Plant-Microbe Interact. 23: 263–272.

Giesman-Cookmyer, D. and Lommel, S. A. 1993. Alanine scanning mutagenesis of a plant virus movement protein identifies three functional domains. Plant Cell 5: 973–982.

Guenoune-Gelbart, D., Elbaum, M., Sagi, G., Levy, A. and Epel, B. L. 2008. *Tobacco mosaic virus* (TMV) replicase and movement protein function synergistically in facilitating TMV spread by lateral diffusion in the plasmodesmal desmotubule of *Nicotiana benthamiana*. Mol. Plant-Microbe Interact. 21: 335–345.

Harries, P.A., Nelson, R.S. 2008. Movement of viruses in plants. *In* Encyclopedia of Virology third edition. Elsevier Academic press, vol. 3: 348-355.

Harries, P. A., Schoelz, J. E. and Nelson, R. S. 2010. Intracellular transport of viruses and their components: utilizing the cytoskeleton and membrane highways. Mol. Plant-Microbe Interact. 23: 1381–1393.

Haupt, S., Cowan, G. H., Ziegler, A., Roberts, A. G., Oparka, K. J. and Torrance, L. 2005. Two plant–viral movement proteins traffic in the endocytic recycling pathway. Plant Cell 17:164–181.

Heinlein, M., Padgett, H. S., Gens, J. S., Pickard, B. G., Casper, S. J., Epel, B. L. and Beachy, R. N. 1998. Changing patterns of localization of the Tobacco mosaic virus movement protein and replicase to the endoplasmic reticulum and microtubules during infection. Plant Cell 10: 1107–1120.

Hirashima, K. and Watanabe, Y. 2001. Tobamovirus replicase coding region is involved in cell-to-cell movement. J. Virol. 75: 8831–8836.

Hirashima, K. and Watanabe, Y. 2003. RNA helicase domain of Tobamovirus replicase executes cell-to-cell movement possibly through collaboration with its nonconserved region J. Virol. 77: 12357–12362.

Iwakawa, H., Mine, A., Hyodo, K., An, M., Kaido, M., Mise K. and Okuno, T. 2011.

Template recognition mechanisms by replicase proteins differ between bipartite positive-strand genomic RNAs of a plant virus. J. Virol. 85:497–509.

Ju, H-J., Brown, J. E., Ye, C-M. and Verchot-Lubicz, J. 2007. Mutations in the central domain of Potato virus X TGBp2 eliminate granular vesicles and virus cell-to-cell movement trafficking. J. Virol. 81: 1899–1911.

Ju, H.-J., Samuels, T.D., Wang, Y.-S., Blancaflor, E., Payton, Mitra, R., M., Krishnamurthy, K., Nelson, R.S. and Verchot-Lubicz, J. 2005. The Potato virus X TGBp2 movement protein associates with the endoplasmic reticulum-derived vesicles during virus infection. Plant Physiol. 138: 1877–1895.

Ju, H-J., Ye, C-M. and Verchot-Lubicz, J. 2008. Mutations analysis of PVX TGBp3 links subcellular accumulation and protein turnover. Virology 375: 103–117.

Kaido, M., Tsuno, Y., Mise, K. and Okuno, T. 2009. Endoplasmic reticulum targeting of the *Red clover necrotic mosaic virus* movement protein is associated with the replication of viral RNA1 but not that of RNA2. Virology 395: 232–242.

Kawakami, S., Watanabe, Y. and Beachy, R. N. 2004. Tobacco mosaic virus infection spreads cell to cell as intact replication complexes. Proc. Natl. Acad. Sci. U.S.A. 101: 6291–6296.

Krishnamurthy, K., Heppler, M., Mitra, R., Blancaflor, E., Payton, M., Nelson, R. S. and Verchot-Lubicz, J. 2003. The *Potato virus X* TGBp3 protein associates with the ER network for virus cell-to-cell movement. Virology 309: 135–151.

Liu, J., Blancaflor, E. B. and Nelson, R. S. 2005. The Tobacco mosaic virus 126-kilodalton protein, a constituent of the virus replication complex, alone or within the complex aligns with and traffics along microfilaments. Plant Physiol. 138: 1853–1865.

Lommel, S. A., Weston-Fina, M., Xiong, Z., Lomonossoff, G.P. 1988. The nucleotide

sequence and gene organization of red clover necrotic mosaic virus RNA-2. Nucleic Acids Res. 16, 8587–8602.

Lough, T. J., Shash, K., Xoconostle-Cázares, B., Hofstra, K. R., Beck, D. L., Balmori, E., Forster, R. L. S. and Lucas, W. J. 1998. Molecular dissection of the mechanism by which potexvirus triple gene block proteins mediate cell-to-cell transport of infectious RNA. Mol. Plant-Microbe Interact. 11: 801–814.

Lucas, W. J. 2006. Plant viral movement proteins: Agents for cell-to-cell trafficking of viral genomes. Virology 344: 169–184.

Melcher, U. (1990). Similarities between putative transport proteins of plant viruses. J. Gen. Virol. 71: 1009–1018.

Melcher, U. 2000. The '30K' superfamily of viral movement proteins. J. Gen. Virol. 81: 257–266.

Mine, A., Hyodo, K., Takeda, A., Kaido, M., Mise, K. and Okuno, T. 2010a. Interactions between p27 and p88 replicase proteins of *Red clover necrotic mosaic virus* play an essential role in viral RNA replication and suppression of RNA silencing via the 480-kDa viral replicase complex assembly. Virology 407: 213–224.

Mine, A., Takeda, A., Taniguchi, T., Taniguchi, H., Kaido, M., Mise, K. and Okuno, T. 2010b. Identification and characterization of the 480-kilodalton template-specific RNA-dependent RNA polymerase complex of *Red clover necrotic mosaic virus*. J. Virol. 84: 6070–6081.

Mitra, R., Krishnamurthy, K., Blancaflor, E., Payton, M., Nelson, R. S. and Verchot-Lubicz, J. 2003. The *Potato virus X* TGBp2 protein association with the endoplasmic reticulum plays a role in but is not sufficient for viral cell-to-cell movement. Virology 312: 35–48.

Mizumoto, H., Iwakawa, H., Kaido, M., Mise, K and Okuno, T. 2006. Cap-independent

translation mechanism of *Red clover necrotic mosaic virus* RNA2 differs from that of RNA1 and is linked to RNA replication. J. Virol. 80: 3781–3791.

Mizumoto, H., Tatsuta, M., Kaido, M., Mise, K and Okuno, T. 2003. Cap-independent translational enhancement by the 3′ untranslated region of *Red clover necrotic mosaic virus* RNA1. J. Virol. 77: 12113–12121.

Mori, M., Mise, K., Okuno, T. and Furusawa, I. 1992. Expression of brome mosaic virus-encoded replicase genes in transgenic tobacco plants. J. Gen. Virol. 73: 169–172.

Nagano, H., Mise, K., Furusawa, I. and Okuno, T. 2001. Conversion in the requirement of coat protein in cell-to-cell movement mediated by the Cucumber mosaic virus movement protein. J. Virol. 75: 8045–8053.

Nagano, H., Okuno, T., Mise, K. and Furusawa, I. 1997. Deletion of the C-terminal 33 amino acids of Cucumber mosaic virus movement protein enables a chimeric Brome mosaic virus to move from cell to cell. J. Virol. 71: 2270–2276.

Nguyen, L., Lucas, W. J., Ding, B., Zaitlin, M. 1996. Viral RNA trafficking is inhibited in replicase-mediated resistant transgenic tobacco plants. Proc. Natl. Acad. Sci. U.S.A. 93: 12643–12647.

Osman, T. A. M., Hayes, R. J. and Buck, K. W. 1992. Cooperative binding of the red clover necrotic mosaic virus movement protein to single-stranded nucleic acids. J. Gen. Virol. 73: 223–227.

Osman, T. A. M., Ingles, P. J., Miller, S. J. and Buck, K. W. 1991a. A spontaneous red clover necrotic mosaic virus mutant with a truncated movement protein. J. Gen.Virol. 72: 1793–1800.

Osman, T. A. M., Miller, S. J., Marriot, A. C. and Buck, K. W. 1991b. Nucleotide sequence of RNA2 of a Czechoslovakian isolate of red clover necrotic mosaic virus. J. Gen. Virol. 72: 213–216.

Osman, T. A. M., Thommes, P. and Buck, K. W. 1993. Localization of a single-stranded RNA-binding domain in the movement protein of red clover necrotic mosaic dianthovirus. J. Gen. Virol. 74: 2453–2457.

Sambade, A., Brandner, K., Hofmann, C., Seemanpillai, M., Mutterer, J. and Heinlein, M. 2008. Transport of TMV movement protein particles associated with the targeting of RNA to plasmodesmata. Traffic 9: 2073–2088.

Sánchez-Navarro, J. and Bol, J. F. 2001. Role of the *Alfalfa mosaic virus* movement protein and coat protein in virus transport. Mol. Plant-Microbe Interact. 14: 1051–1062.

Sit, T. L., Vaewhongs, A. A. and Lommel, S. A. 1998. RNA-mediated trans-activation of transcription from a viral RNA. Science 281: 829–832.

Tagami, Y. and Watanabe, Y. 2007. Effects of brefeldin A on the localization of *Tobamovirus* movement protein and cell-to-cell movement of the virus. Virology 361: 133–140.

Takeda, A., Kaido, M., Okuno, T. and Mise, K. 2004. The C terminus of the movement protein of *Brome mosaic virus* controls the requirement for coat protein in cell-to-cell movement and plays a role in long-distance movement. J. Gen. Virol. 85: 1751–1761.

Takeda, A., Tsukuda, M., Mizumoto, H., Okamoto, K., Kaido, M., Mise, K. and Okuno, T. 2005. A plant RNA virus suppresses RNA silencing through viral RNA replication. EMBO J. 24: 3147–3157.

Tamai, A. and Meshi, T. 2001a. Tobamoviral movement protein transiently expressed in a single epidermal cell functions beyond multiple plasmodesmata and spreads multicellularly in an infection-coupled manner. Mol. Plant-Microbe Interact. 14: 126–134.

Tamai, A. and Meshi, T. 2001b. Cell-to-cell movement of *Potato virus X*: The role of

p12 and p8 encoded by the second and third open reading frames of the triple gene block. Mol. Plant-Microbe Interact. 14: 1158–1167.

Tatsuta, M., Mizumoto, H. Kaido, M. Mise, K. and Okuno, T. 2005. The *Red clover necrotic mosaic virus* RNA2 *trans*-activator is also a *cis*-acting RNA2 replication element. J. Virol. 79: 978–986.

Tilsner, J., Cowan, G. H., Roberts, A. G., Chapman, S. N., Ziegler, A., Savenkov, E. and Torrance, L. 2010. Plasmodesmal targeting and intercellular movement of potato mop-top pomovirus is mediated by a membrane anchored tyrosine-based motif on the luminal side of the endoplasmic reticulum and the C-terminal transmembrane domain in the TGB3 movement protein. Virology 402: 41–51.

Tremblay, D., Vaewhongs, A. A., Turner, K. A., Sit, T. L. and Lommel, S. A. 2005. Cell wall localization of *Red clover necrotic mosaic virus* movement protein is required for cell-to-cell movement. Virology 333: 10–21.

Verchot-Lubicz, J., Torrance, L., Solovyev, A. G., Morozov, S. Y., Jackson, A. O. and Gilmer, D. 2010. Varied movement strategies employed by triple gene block-encoding viruses. Mol. Plant-Microbe Interact. 23: 1231–1247.

Verchot-Lubicz, J., Ye, C-M. and Bamunusinghe, D. 2007. Molecular biology of potexviruses: recent advances. J. Gen. Virol. 88: 1643–1655.

Waigmann, E., Ueki, S., Trutnyeva, K. and Citovsky, V. 2004. The ins and outs of nondestructive cell-to-cell and systemic movement of plant viruses. Crit. Rev. Plant Sci. 23: 195–250.

Wang, H-L., Wang, Y., Giesman-Cookmyer, D., Lommel, S. A. and Lucas, W. J. 1998. Mutations in viral movement protein alter systemic infection and identify an intercellular barrier to entry into the phloem long-distance transport system. Virology 245: 75–89.

Wright, K. M., Wood, N. T., Roberts, A. G., Chapman, S., Boevink, P., MacKenzie, K. M. and Oparka, K. J. 2007. Targeting of TMV movement protein to plasmodesmata requires the actin/ER network: evidence from FRAP. Traffic 8: 21–31.

Xiong, Z., Kim, K.H., Giesman-Cookmeyer, D. and Lommel, S.A. 1993. The roles of the Red clover necrotic mosaic virus capsid and cell-to-cell movement proteins in systemic infection. Virology 192, 27–32.

Xiong, Z. and Lommel, S.A. 1991. Red clover necrotic mosaic virus infectious transcripts synthesized *in vitro*. Virology 182, 388–392.

Figure legends

Fig. 1. (A) Genome maps of *Red clover necrotic mosaic virus* (RCNMV) and derivative constructs used in this study. Plasmids containing the prefix 'pUC' and pRNA2fsMP were digested with SmaI and used as templates for *in vitro* transcription. Plasmids containing the prefix 'pUB' were used for microprojectile bombardment experiments. Plasmids containing the prefix 'pBIC' were used for agroinfiltration. Others were used for protein expression in *E. coli*. Shaded boxes labeled with GFP denote the open reading frame (ORF) of synthetic green fluorescent protein (Chiu et al., 1996). Light-shaded boxes denote ORFs of RCNMV. The dashed box denotes an untranslated MP ORF. Black boxes denote the hemagglutinin (HA) tag. Boxes with slanted lines denote the myc tag and boxes with horizontal stripes denote 6 × histidine tag. fs is the four-nucleotide insertion for a frameshifting mutation. Bold lines denote the RCNMV untranslated sequences. Key: T7, T7 promoter; T7 ter, T7 terminator; Pro, *Cauliflower mosaic virus* (CaMV) 35S promoter; Ter, CaMV terminator; SmaI, SmaI recognition sequence; MPdC70, C-terminal 70 amino acid-deleted MP. (B) Surface probability plot for RCNMV MP and amino acid sequence of the C-terminal 70 amino acids of the protein. The surface probability for RCNMV MP was analyzed using the method of Emini et al. (1985). Black stars indicate amino acids with charged side chains. White stars indicate amino acids with uncharged polar side chains.

Fig. 2. Effects of C-terminal region deletion of RCNMV MP on cell-to-cell movement of the encoding recombinant viruses. Each of an i*n vitro* transcript of pUCR1-MsG (R1-MsG), or pUCR1-MdCnsG (n = 60, 66, 67, 68, 69 and 70, R1-MdCnsG), or pUCR1-Md248sG (R1-Md248sG) was mixed with an *in vitro* transcript of pRNA2fsMP (R2fsMP) and was mechanically inoculated onto young leaves of *Nicotiana benthamiana*. (A) Representative images of fluorescent foci at 30 h post inoculation by epifluorescence microscopy. Scale bar = 50 μm. (B) Percentage of fluorescent foci composed of multiple cells detected by epifluorescence microscopy at 30 h post inoculation. Data shown are the total of three replicates for the assays.

Fig. 3. Deletion of the C-terminal region of RCNMV MP gradually impairs cytoplasmic aggregate formation. A mixture of R1-MsG and R2fsMP, or each of R1-MdCnsG (n = 66 to 70) and R2fsMP was mechanically inoculated to young leaves of *N. benthamiana*. (A) Representative epifluorescence microscopy images of fluorescent cells 14 h after inoculation. Scale bar = 20 μm. (B) Percentage of fluorescent cells with cytoplasmic punctate structures detected by epifluorescence microscopy at 14 h post inoculation. Data shown are the total of three replicates for the assays. (C) Representative confocal microscopy images at 14 or 27 h post inoculation. Images are mergers of differential interference contrast (DIC) and GFP channels and present confocal projections composed of 20 optical sections taken at 1 μm intervals, reaching from the surface to the middle of epidermal cells. Scale bar = 10 μm. (D) *N. benthamiana* leaves were infiltrated with the *Agrobacterium* cultures containing pBIC/ER-mCherry (ER marker) and mechanically inoculated 21 h later with a mixture of R1-MdC70sG and R2fsMP. Representative confocal microscopy images at 27 h post inoculation. Images are mergers of DIC and GFP and RFP channels and present confocal projections composed of 10 optical sections taken at 1 μm intervals, covering the surface of epidermal cells. Scale bar = 10 μm.

Fig. 4. Effects of C-terminal 70 amino acid deletion of RCNMV MP on accumulation of recombinant viral RNAs and the MP-GFPs in the *N. benthamiana* protoplasts at 20 h post inoculation. (A) Representative confocal images of *N. benthamiana* protoplasts inoculated with a mixture of R1-MsG and R2fsMP or R1-MdC70sG and R2fsMP. Images are mergers of differential interference contrast (DIC) and GFP channels and present confocal projections composed of 15 optical sections taken at 1 μm intervals, reaching from the surface to the middle of protoplasts. (B) Negative-strand viral RNA accumulation level in the protoplasts. Total RNA (2 μg) was loaded to each lane. Negative-strand RNA1 and RNA2 were detected using specific riboprobes; rRNA was an ethidium bromide-stained agarose gel image of 1 μg total RNA as the loading control. Numbers below images represent relative accumulation (means ± SE) of viral RNAs using the Image Gauge program (Fuji Film), calculated from three independent experiments. * indicates a not significant ($P < 0.05$; Student's t test) difference relative

to viral RNA accumulation level in the protoplasts inoculated with R1-MsG + R2fsMP. (C) MP-GFP and MPdC70-GFP accumulation in the protoplasts. Proteins extracted from 2 x 10^5 protoplasts were loaded in each lane. MP-GFP and MPdC70-GFP were detected using rabbit polyclonal antibodies against GFP. RubL is a Coomassie brilliant blue-stained gel image of proteins extracted from 2 x 10^5 protoplasts showing the large subunit of Rubisco proteins. Numbers below images represent relative accumulation (means ± SE) of the proteins using the Image Gauge program (Fuji Film), calculated from three independent experiments. ** indicates a significant ($P < 0.05$; Student's t test) difference relative to the protein accumulation level in the protoplasts inoculated with R1-MsG + R2fsMP.

Fig. 5. Deletion of C-terminal 70 amino acids of RCNMV MP did not affect the plasmodesmata size exclusion limit enlargement ability in *N. benthamiana*. Pictures are representative images of fluorescent foci for each bombardment assay. Gold particles were coated with a mixture of pUBsGFP and each of pUBRMP, pUBRMPdC70, or pUBP35 plasmids. At two days post bombardment, fluorescent foci were observed by epifluorescence microscopy. Data shown are the total of six replicates for the assays.

Fig. 6. Deletion of C-terminal 70 amino acids of RCNMV MP does not affect its RNA binding ability. Indicated amounts of $(His)_6$-tagged recombinant MP and MPdC70 that had been purified from *E. coli* using an Ni-NTA column were incubated with [α-^{32}P]UTP-labeled *in vitro* transcripts of a RCNMV RNA2 fragment (200 nucleotides). RNA–protein complexes were loaded on 0.75% agarose gel and electrophoresed. The gel was dried and radioactive signals were detected using FLA-5100 (Fuji Film).

Fig. 7. Immunoprecipitation assay of RCNMV MP and MPdC70. HA- or myc-tagged MP or MPdC70 were expressed in *N. benthamiana* leaves using agroinfiltration. Protein extracts from *Agrobacterium*-infiltrated leaves expressing viral proteins were subjected to western blotting (upper two panels, Input) to evaluate the accumulation level of each HA- or myc-tagged proteins, or subjected to immunoprecipitation with anti-myc antibody followed by western blotting using anti-HA antibody (IP: myc, WB: HA). GFP-HA shows HA-tagged GFP, used as the negative control. P35 shows negative

control vector pBICP35. RubL is a Coomassie brilliant blue-stained gel image showing the large subunit of Rubisco proteins. The asterisk indicates the degradation products of GFP-HA.

Acknowledgements

We thank Dr. S. A. Lommel for providing plasmids R1-MP:GFP, pRC1|G, and pRC2|G and Dr. J. Wellink for providing the plasmid pUC-mGFP5-ER. We are also grateful to Dr. H. Iwakawa and Dr. A. Mine for helpful discussion. This study was supported in part by a Grant-in-Aid (19580046) for Scientific Research C and a Grant-in-Aid (22580047) for Scientific Research C from the Japan Society for the Promotion of Science.

Fig.1 Kaido et al., 2011

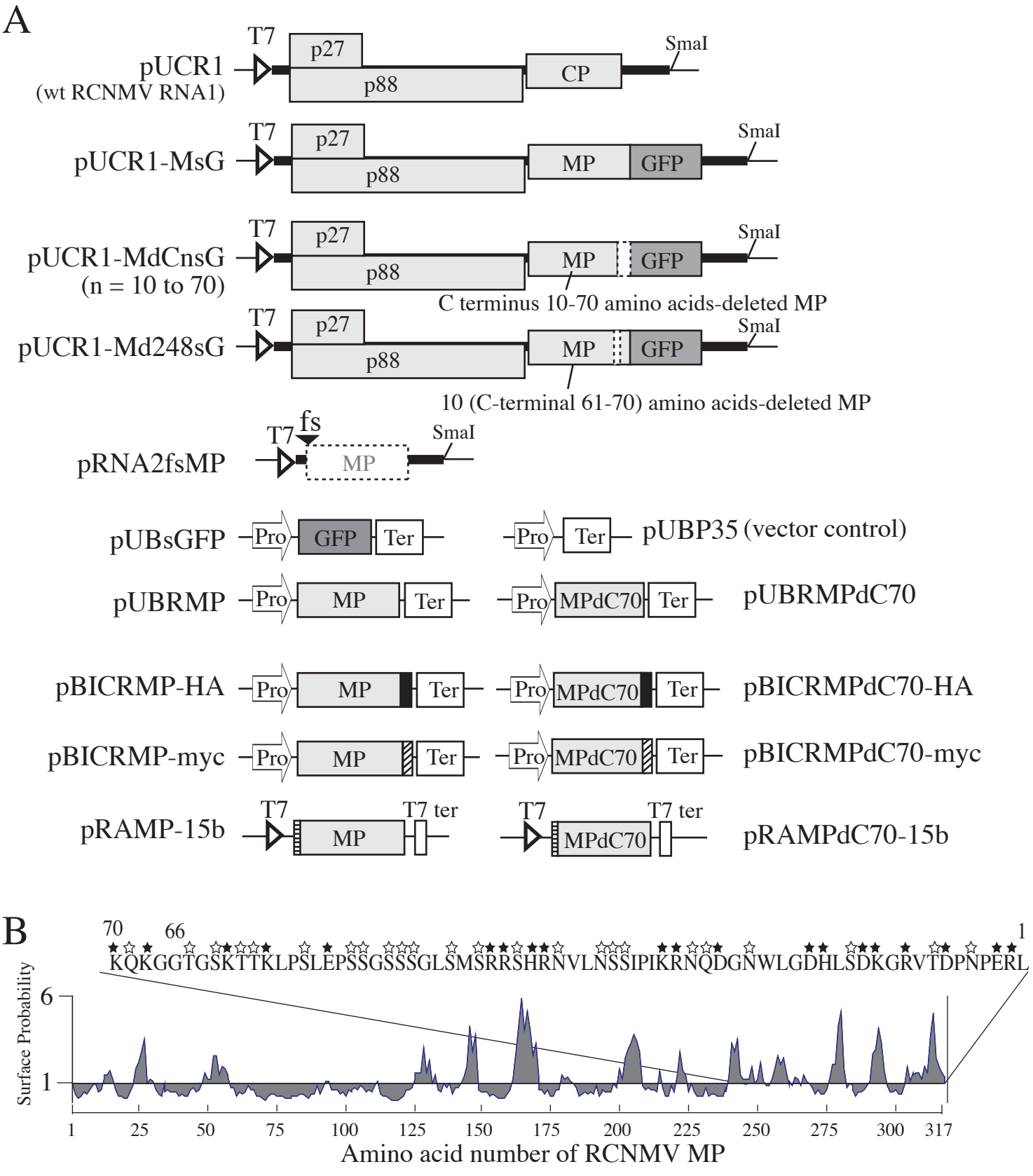

Fig. 2 Kaido et al., 2011

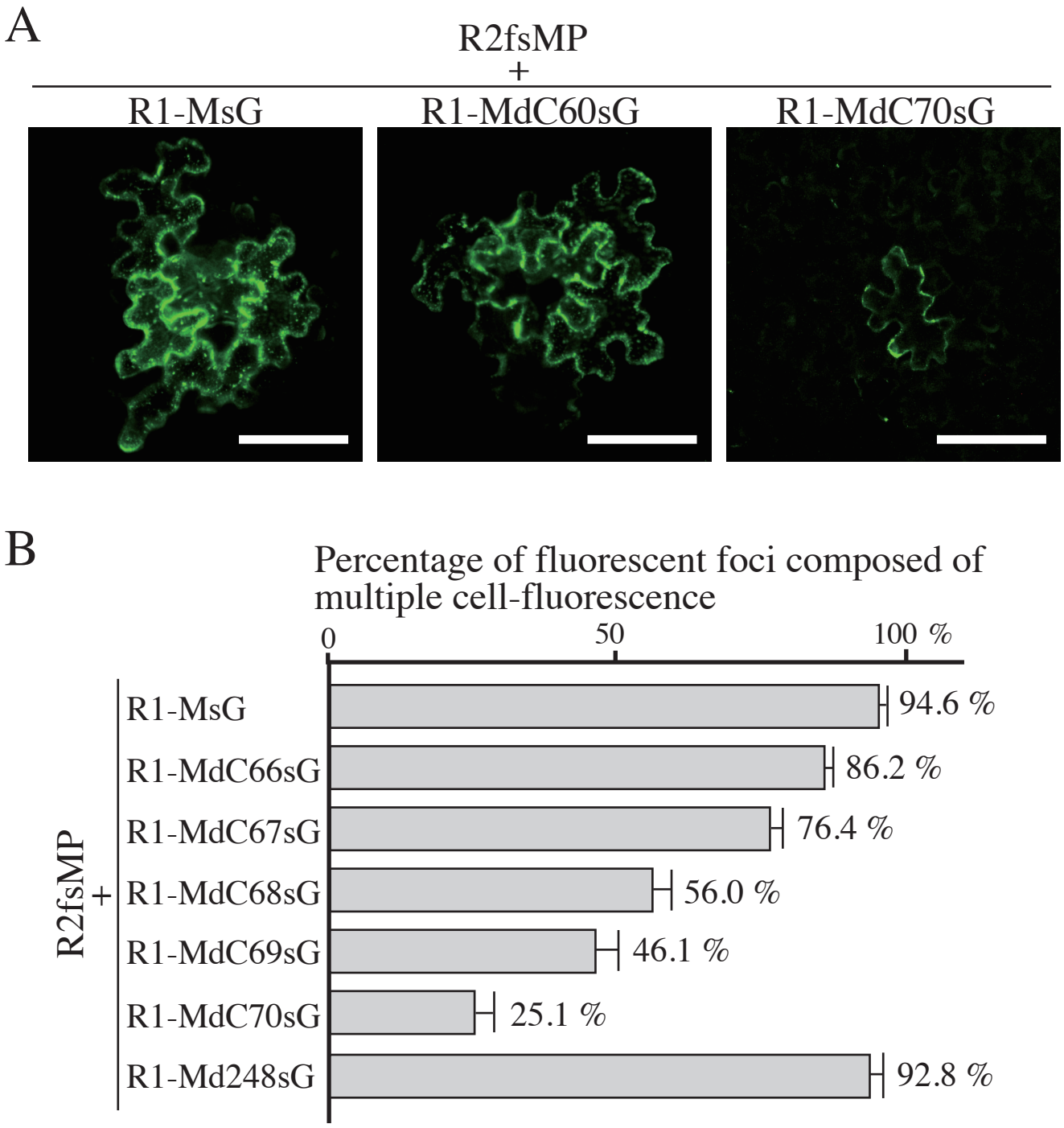

Fig. 3 Kaido et al., 2011

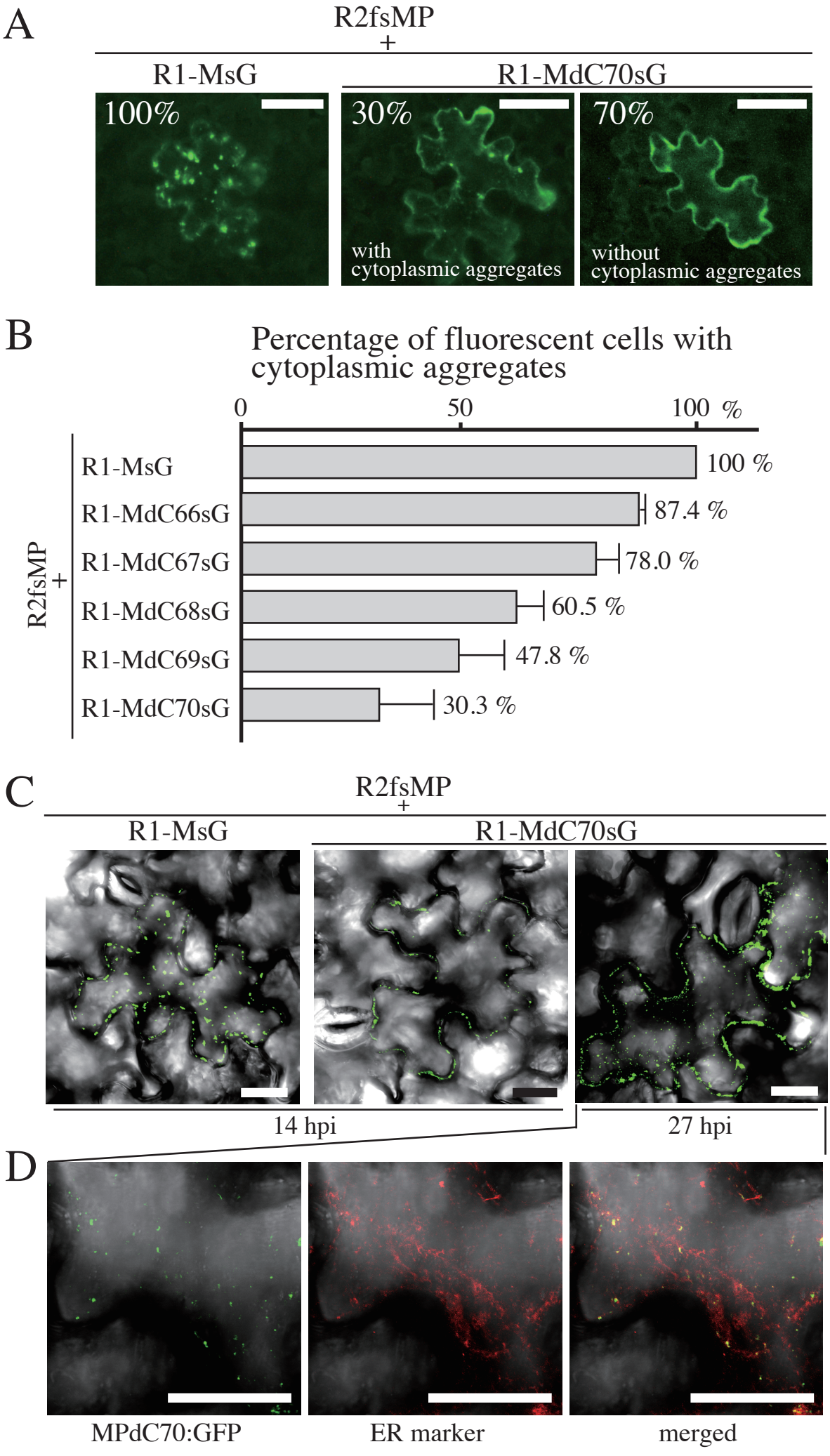

Fig. 4 Kaido et al., 2011

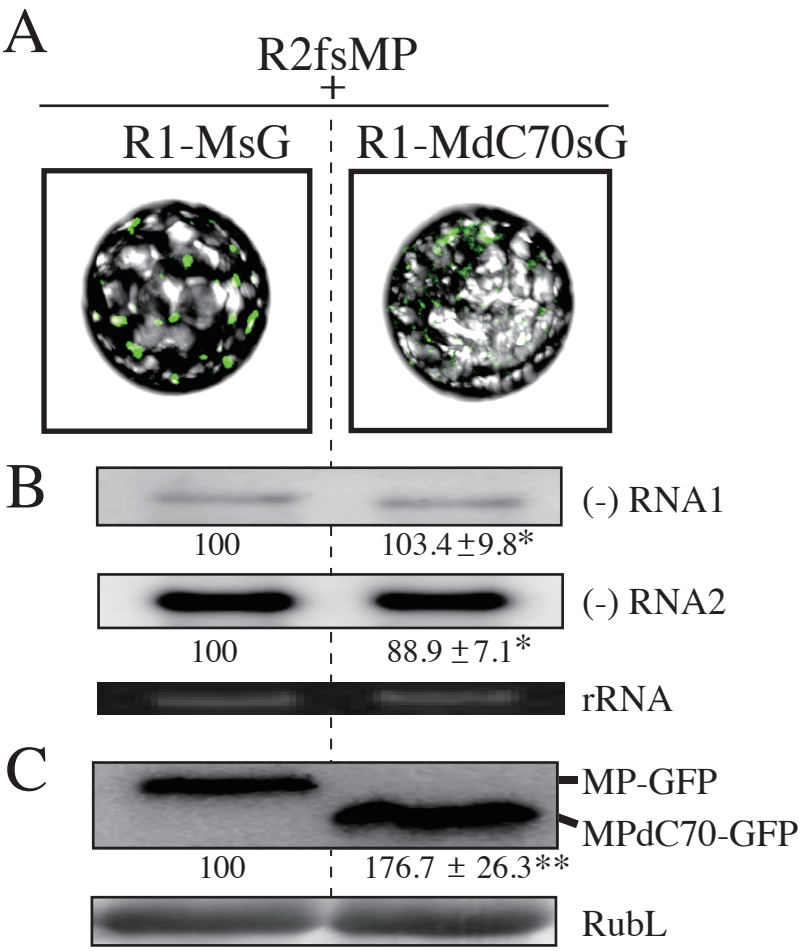

Fig. 5 Kaido et al., 2011

GFP +

wt MP | MPdC70 | P35 (vector control)

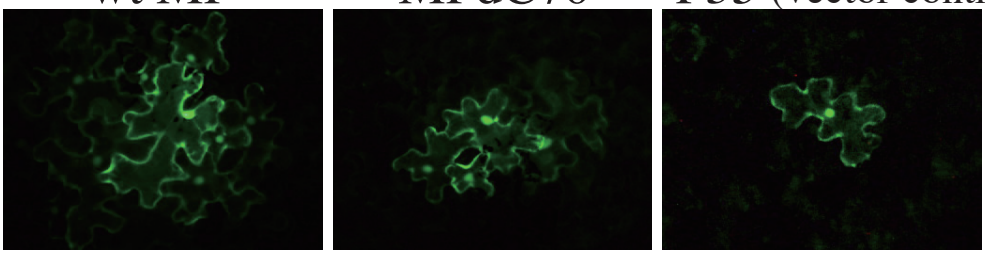

Percentage of multicellular fluorescence

GFP + wt MP	54.7	(n = 225)
GFP + MPdC70	53.7	(n = 376)
GFP + P35	8.3	(n = 288)

Fig. 6 Kaido et al., 2011

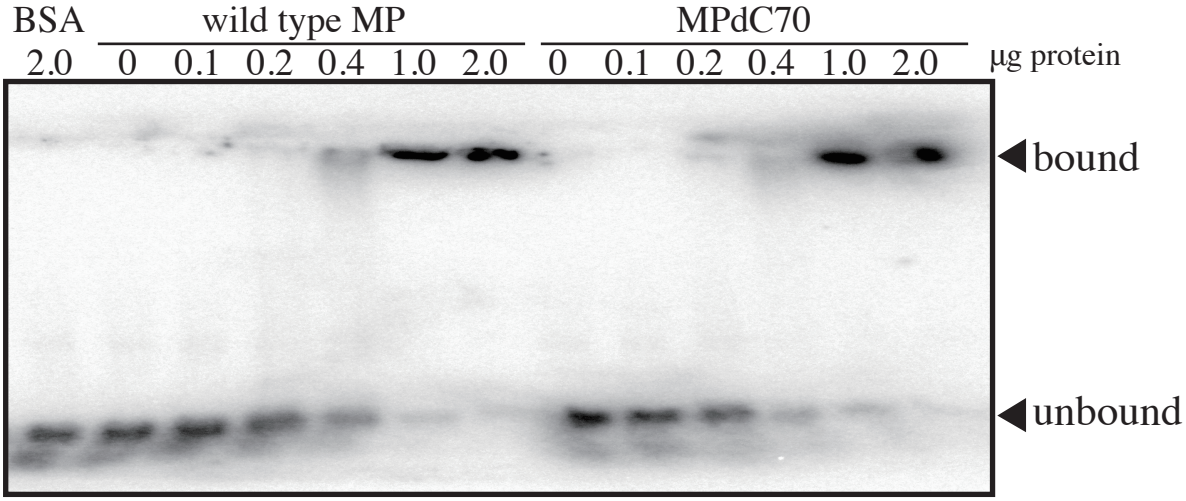

Fig. 7 Kaido et al., 2011